

Effects of oxygen vacancies on the electronic structure of the (LaVO₃)₆/SrVO₃ superlattice: a computational study

Qingqing Dai, Ulrich Eckern, Udo Schwingenschlögl

Angaben zur Veröffentlichung / Publication details:

Dai, Qingqing, Ulrich Eckern, and Udo Schwingenschlögl. 2018. "Effects of oxygen vacancies on the electronic structure of the (LaVO₃)₆/SrVO₃ superlattice: a computational study." *New Journal of Physics* 20 (7): 073011. <https://doi.org/10.1088/1367-2630/aac486>.

PAPER • OPEN ACCESS

Effects of oxygen vacancies on the electronic structure of the $(\text{LaVO}_3)_6/\text{SrVO}_3$ superlattice: a computational study

To cite this article: Qingqing Dai *et al* 2018 *New J. Phys.* **20** 073011

View the [article online](#) for updates and enhancements.

Related content

- [Lattice relaxation and ferromagnetic character of \$\(\text{LaVO}_3\)_m/\text{SrVO}_3\$ superlattices](#)
Cosima Schuster, Ulrike Lüders, Raymond Frésard *et al.*
- [Kondo effect goes anisotropic in vanadate oxide superlattices](#)
H Rotella, A Pautrat, O Copie *et al.*
- [Unusual ferromagnetic \$\text{YMnO}_3\$ phase in \$\text{YMnO}_3/\text{La}_2/3\text{Sr}1/3\text{MnO}_3\$ heterostructures](#)
Carmine Autieri and Biplab Sanyal



IOP | ebooks™

Bringing you innovative digital publishing with leading voices to create your essential collection of books in STEM research.

Start exploring the collection - download the first chapter of every title for free.



PAPER

Effects of oxygen vacancies on the electronic structure of the $(\text{LaVO}_3)_6/\text{SrVO}_3$ superlattice: a computational study

OPEN ACCESS

RECEIVED

22 November 2017

REVISED

27 April 2018

ACCEPTED FOR PUBLICATION

14 May 2018

PUBLISHED

4 July 2018

Original content from this work may be used under the terms of the [Creative Commons Attribution 3.0 licence](#).

Any further distribution of this work must maintain attribution to the author(s) and the title of the work, journal citation and DOI.

Qingqing Dai¹, Ulrich Eckern²  and Udo Schwingenschlög¹ ¹ King Abdullah University of Science and Technology (KAUST), Physical Science and Engineering Division (PSE), Thuwal 23955-6900, Saudi Arabia² Institut für Physik, Universität Augsburg, 86135 Augsburg, GermanyE-mail: udo.schwingenschlogl@kaust.edu.sa**Keywords:** superlattice, magnetism, ordering, defectSupplementary material for this article is available [online](#)

Abstract

By means of first principles calculations, we comprehensively investigate the stability of O vacancies at the different possible sites in the $(\text{LaVO}_3)_6/\text{SrVO}_3$ superlattice and their effect on the electronic structure. Formation energy calculations demonstrate that O vacancies are formed most easily in or close to the SrO layer. We show that O vacancies at these energetically favorable sites conserve the semiconducting character of the superlattice by reducing V^{4+} ions next to the SrO layer to V^{3+} ions, while all other sites result in a metallic character.

1. Introduction

O vacancies in transition metal oxides are becoming increasingly critical in device applications, since they act as electron donors and therefore can strongly perturb the electronic structure [1–3]. On the other hand, as the O vacancy concentration may be reversibly controlled by an external electric field or by epitaxial strain, the electronic conductivity and magnetism of transition metal oxides can be tuned without introducing other impurities [4, 5]. Numerous experimental and theoretical works have investigated the formation and diffusion of O vacancies (and the induced effects on the electronic and magnetic properties) in transition metal oxide thin films [5–8] and heterostructures [9–11], while the role of O vacancies in superlattices is still a developing field. For the $\text{LaAlO}_3/\text{SrTiO}_3$ heterostructure (of non-magnetic insulators), for example, the consequences of O vacancies for the formation of a two-dimensional electron gas or even superconductivity at the interface, as found experimentally, have been studied in [12–15]. O vacancies also play a decisive role for the magnetic ordering in this heterostructure [15, 16].

$\text{LaVO}_3/\text{SrVO}_3$ superlattices with different periodicities are attracting a lot of interest in recent years, particularly due to magnetic features that do not exist in the bulk compounds [17–22]. It also has been reported that the saturation magnetization of $(\text{LaVO}_3)_m/\text{SrVO}_3$ superlattices is larger for even than for odd values of m [18]. The key for understanding the experimental situation may be the observation of simultaneous appearance of both V^{3+} ions (as in bulk LaVO_3) and V^{4+} ions (as in bulk SrVO_3) at the interface of the $(\text{LaVO}_3)_6/(\text{SrVO}_3)_3$ superlattice in [22]. Under the assumption that there are no O vacancies, first principles calculations show that these V^{3+} and V^{4+} ions form a checkerboard pattern adjacent to the SrO layer [23]. However, in a real sample, O vacancies are inevitable during the growth process [24], which may affect the electronic reconstruction of the V ions and, thus, the properties of the superlattice. In addition, it can be expected that the location of an O vacancy with respect to the SrO layer is important for its influence on the electronic structure. In order to clarify the role of O vacancies in the $(\text{LaVO}_3)_6/\text{SrVO}_3$ superlattice, which has been investigated experimentally in [18], we thus introduce in the present work such vacancies in different distances from the SrO layer and study their stability. This will allow us to determine the induced charge transfer as well as the effects on the electronic properties.

2. Methodology

Spin polarized first principles calculations are performed employing the projector augmented wave method [25, 26] (pseudopotentials with the following cores: He for O, Ne $3s^2$ for V, Ar $3d^{10}$ for Sr, and Kr $4d^{10}$ for La) of the Vienna *ab initio* simulation package [27–30]. The generalized gradient approximation (Perdew–Burke–Ernzerhof [31, 32]) is adopted for the exchange–correlation functional and the electronic correlations in the V $3d$ orbitals are taken into account by an effective onsite interaction parameter of 3 eV [33]. The cut-off energy of the plane wave basis is chosen as 500 eV. We have checked that a higher cut-off energy of 650 eV results for the pristine $(\text{LaVO}_3)_6/\text{SrVO}_3$ superlattice in a total energy difference of less than 0.05 eV and a change in the band gap of less than 0.01 eV. The Brillouin zone is sampled on a $9 \times 9 \times 1$ k-mesh, for which we have confirmed convergence. The total energy of the self-consistency calculations is converged to 1×10^{-5} eV and the atomic positions are relaxed until the forces on all atoms have declined below $0.02 \text{ eV } \text{\AA}^{-1}$.

We form a single O vacancy in the $(\text{LaVO}_3)_6/\text{SrVO}_3$ superlattice by removing 1 out of the 42 O atoms. This represents a sufficiently low defect concentration that only the atomic coordinates have to be relaxed, while the lattice constants can be adopted from the pristine superlattice without relaxation.

However, the shortest distance between O vacancies (through the periodic boundary conditions) is only 5.5 Å in our simulation cell, implying that the interaction between the defects is not yet fully negligible. Lowering the defect concentration, on the other hand, would require a larger simulation cell, which is computationally not treatable as a consequence of a very slow convergence behavior. A superlattice with thinner LaVO_3 slab also is not an alternative, because the experimental situation would no longer be modeled and the interfaces at the two ends of the slab would start interacting. Due to the epitaxial strain present in the $(\text{LaVO}_3)_6/\text{SrVO}_3$ superlattice, the magnetic order is found to be A-type antiferromagnetic throughout the superlattice except for ferromagnetic coupling of the two VO_2 layers next to the SrO layer, which is in agreement with the results reported in [27]. For comparison, we also study O deficient bulk LaVO_3 using the lattice constants of the superlattice and enforcing A-type antiferromagnetic ordering. The formation energy of an O vacancy is calculated as

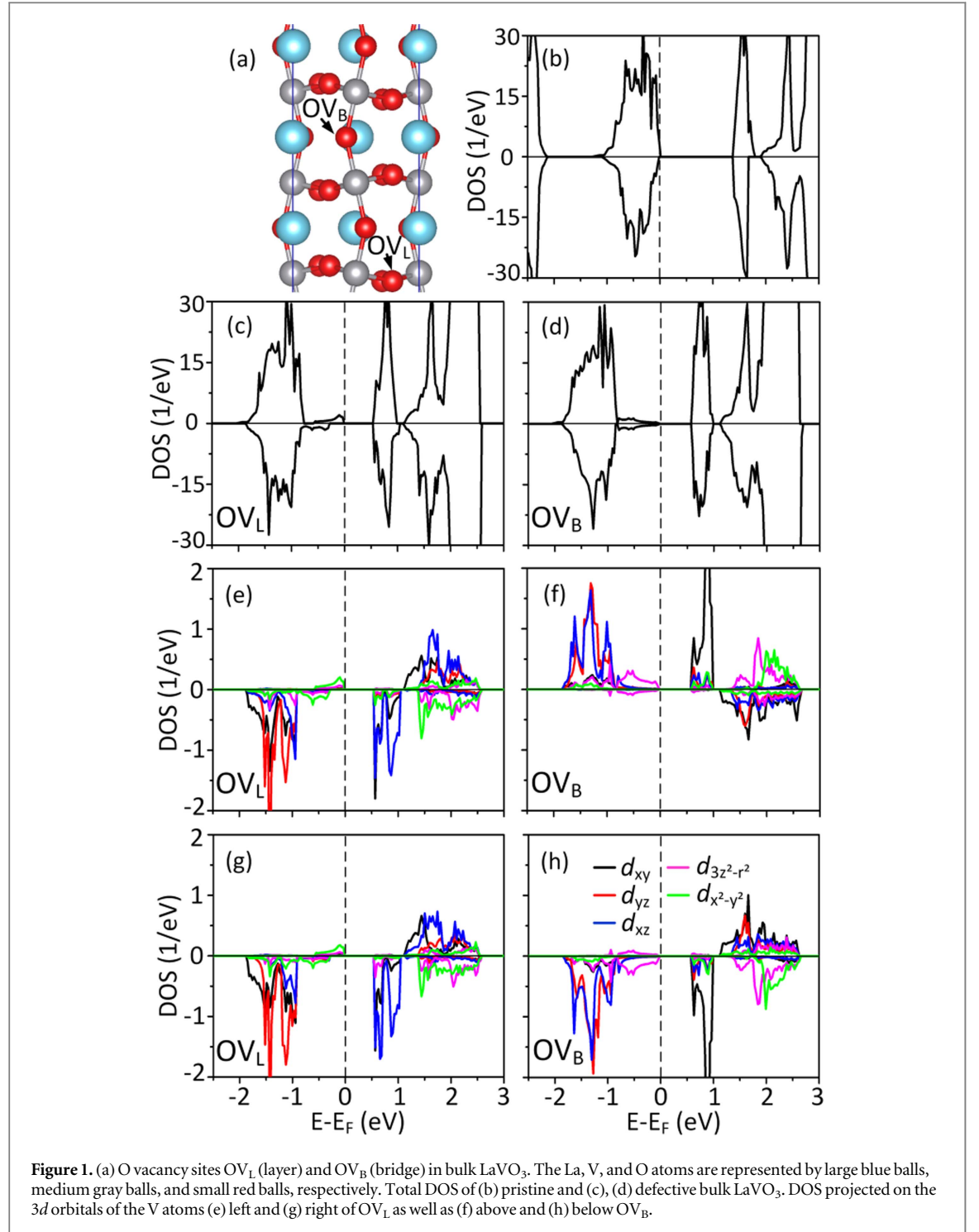
$$E_f = E_{\text{defective}} + \frac{1}{2}E_{\text{O}_2} - E_{\text{pristine}}, \quad (1)$$

where $E_{\text{defective}}$ is the total energy of the O deficient superlattice, E_{O_2} the total energy of a gas phase O_2 molecule (triplet ground state), and E_{pristine} the total energy of the pristine superlattice.

3. Results and discussion

Our calculations for bulk LaVO_3 result in a band gap of 1.39 eV, which is close to the experimental value of 1.1 eV as reported in [34]. The two inequivalent O vacancy sites in bulk LaVO_3 are shown in figure 1(a): OV_L is located in the VO_2 layer and OV_B in the LaO layer (forming a bridge between VO_2 layers). The formation energy of OV_L (5.54 eV) is found to be higher than that of OV_B (5.39 eV), which suggests that O vacancies favor the LaO layer. Figures 1(c) and (d) show the density of states (DOS) obtained for OV_L and OV_B in bulk LaVO_3 , respectively. In both cases the semiconducting state is maintained with a band gap of 0.60 eV. As compared to the DOS of pristine bulk LaVO_3 (band gap 1.39 eV), see figure 1(b), additional states appear above the valence band and strongly reduce the size of the band gap. Analysis of the DOS projected on the $3d$ orbitals of the V atoms located next to an O vacancy, see figures 1(e)–(h), shows that e_g states ($d_{x^2-y^2}$ in the case of OV_L and $d_{3z^2-r^2}$ in the case of OV_B) form the valence band edge. The magnetic moments of these V atoms increase slightly from $1.82 \mu_B$ (pristine bulk LaVO_3) to $1.96 \mu_B$. The occupation of e_g states can be attributed to transfer of excess charge (from the O vacancy) to the neighboring V ions. We find that next to OV_B each V atom gains 0.45 electrons and each La atom gains 0.19 electrons. Next to OV_L the V atoms also gain 0.45 electrons and the two closest La atoms gain 0.06 and 0.13 electrons, respectively. It should be noted that Bader charges tend to underestimate charge transfers.

We consider for the $(\text{LaVO}_3)_6/\text{SrVO}_3$ superlattice all inequivalent O vacancy sites: four sites in each of the VO_2 layers L1 to L4 (OV_L), see figure 2(a), and two sites in each LaO layer in between them (OV_B). The O vacancy formation energies obtained for these sites are summarized in figure 2(b). In the bulk-like region of the superlattice (L3, L4) the values are similar to our results for OV_L and OV_B in bulk LaVO_3 , compare the dotted lines in figure 2(b). They decrease gradually when we approach layer L1, showing that O vacancies are formed more easily towards the interface of the superlattice. A similar behavior has been reported in [35] for the $\text{LaAlO}_3/\text{SrTiO}_3$ interface. Interestingly, we find a change in the electronic character of the superlattice as function of the distance of the O vacancy from the SrO layer, see figure 2(c): while O vacancies in the bulk-like region of the superlattice give rise to metallic states, those located close to the interface (layer L2 are closer) conserve the original semiconducting state. In addition, within the semiconducting regime, the band gap grows gradually towards the interface.



We first analyze the metallic state of the defective superlattice. Since the different O vacancy sites of this regime, compare figure 2, behave similarly, we study as first example an O vacancy in layer L3 in more detail. The total DOS and band structure obtained for this case are illustrated in figures 3(a) and (b), respectively. The pristine $(LaVO_3)_6/SrVO_3$ superlattice is predicted to exhibit a band gap of 0.70 eV, while figure 3 shows for the superlattice with O vacancy in layer L3 a significant number of electronic states at the Fermi energy (mainly spin majority states, but also spin minority states). In figure 4 further insight is provided by projecting the DOS on the 3d orbitals of individual V atoms in layers L1 and L3. In the case of the pristine $(LaVO_3)_6/SrVO_3$ superlattice, V^{3+} ions (sites V1b and V1c) and V^{4+} ions (sites V1a and V1d) form a checkerboard pattern next to the SrO layer. Everywhere else we have V^{3+} ions. In the case of defective bulk $LaVO_3$, as discussed earlier, the excess charge enters mainly the $d_{x^2-y^2}$ or $d_{3z^2-r^2}$ orbitals of the two V ions next to the O vacancy, whereas in the superlattice a substantial part of this charge does not stay at sites V3c and V3d but is transferred to a V^{4+} ion at the interface (site V1d, see figure 4(d)), resulting in a partially occupied band. Correspondingly, the $d_{x^2-y^2}$

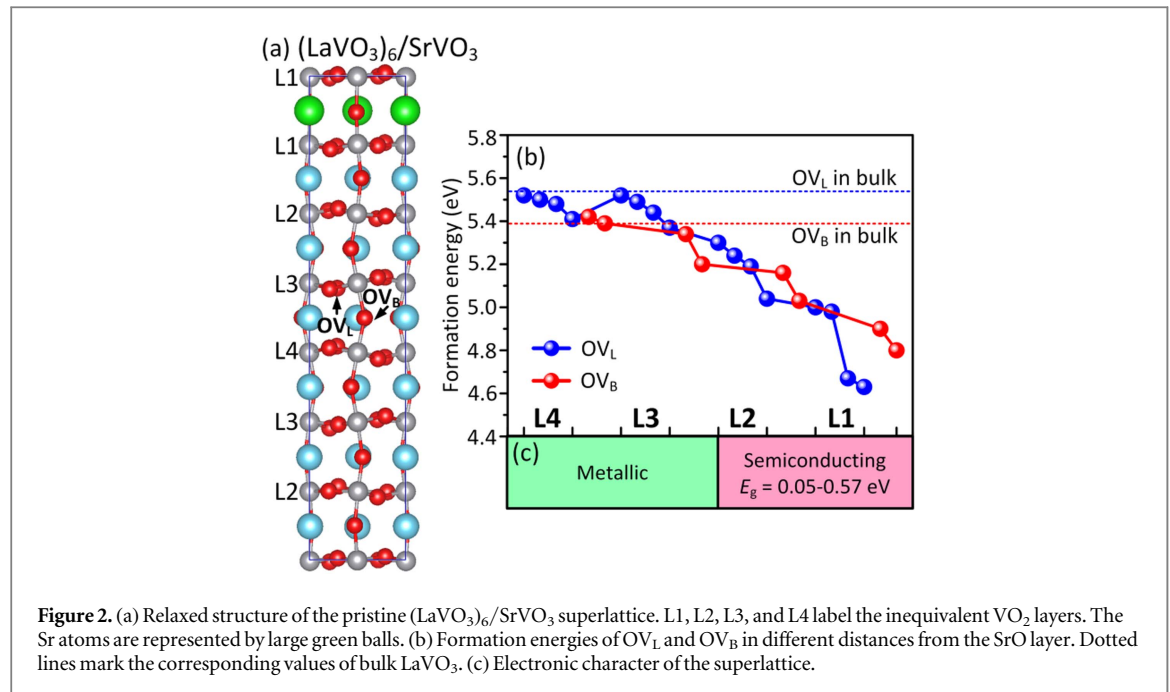


Figure 2. (a) Relaxed structure of the pristine (LaVO₃)₆/SrVO₃ superlattice. L1, L2, L3, and L4 label the inequivalent VO₂ layers. The Sr atoms are represented by large green balls. (b) Formation energies of OV_L and OV_B in different distances from the SrO layer. Dotted lines mark the corresponding values of bulk LaVO₃. (c) Electronic character of the superlattice.

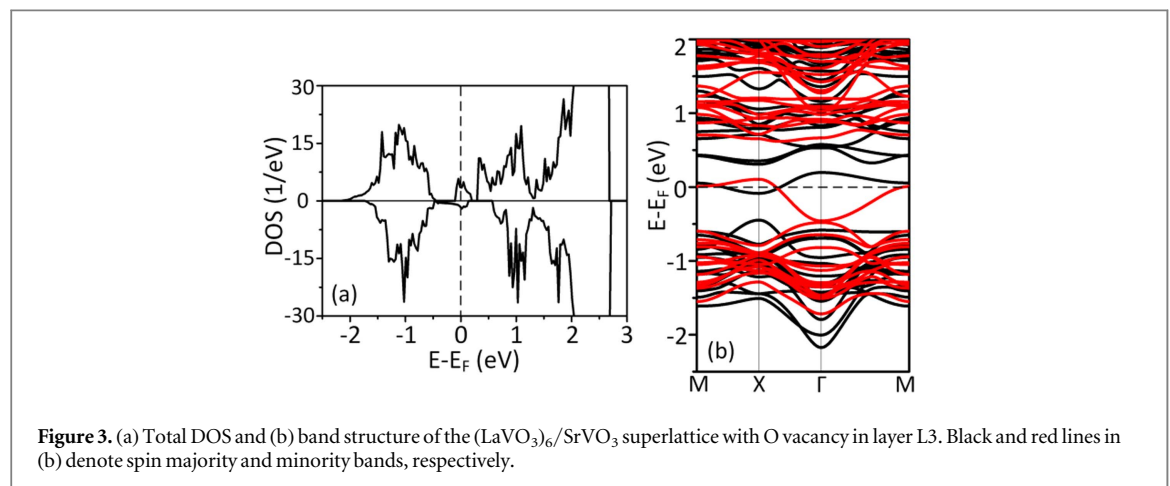
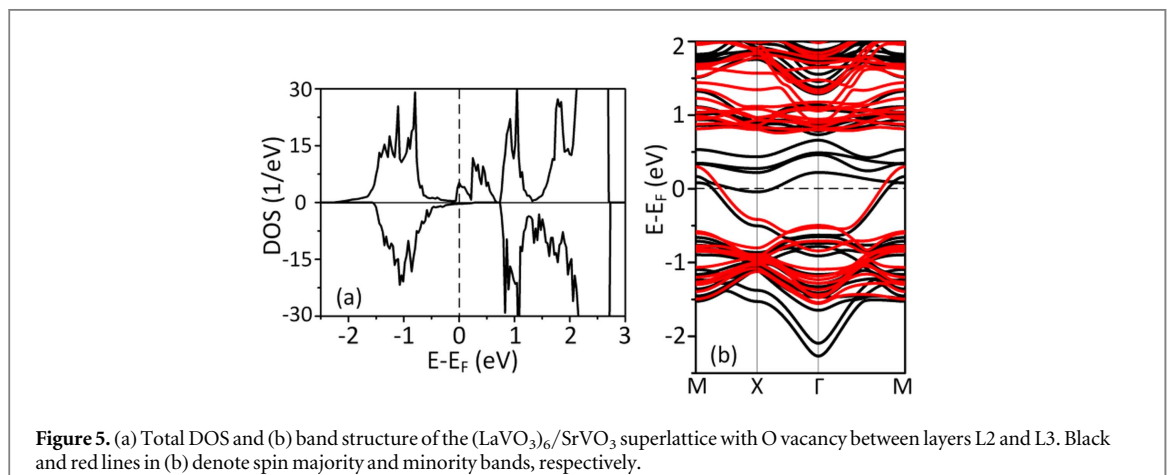
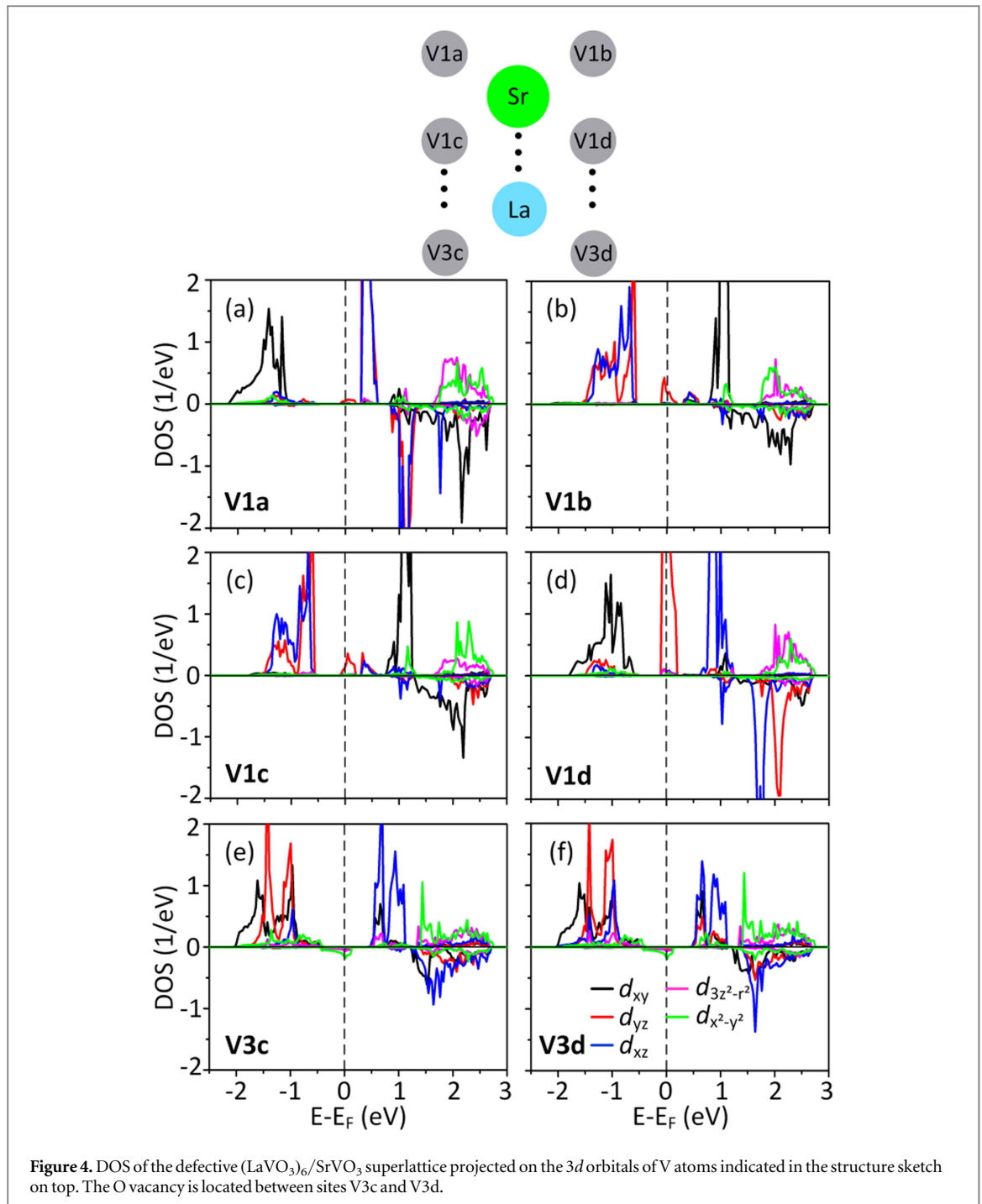


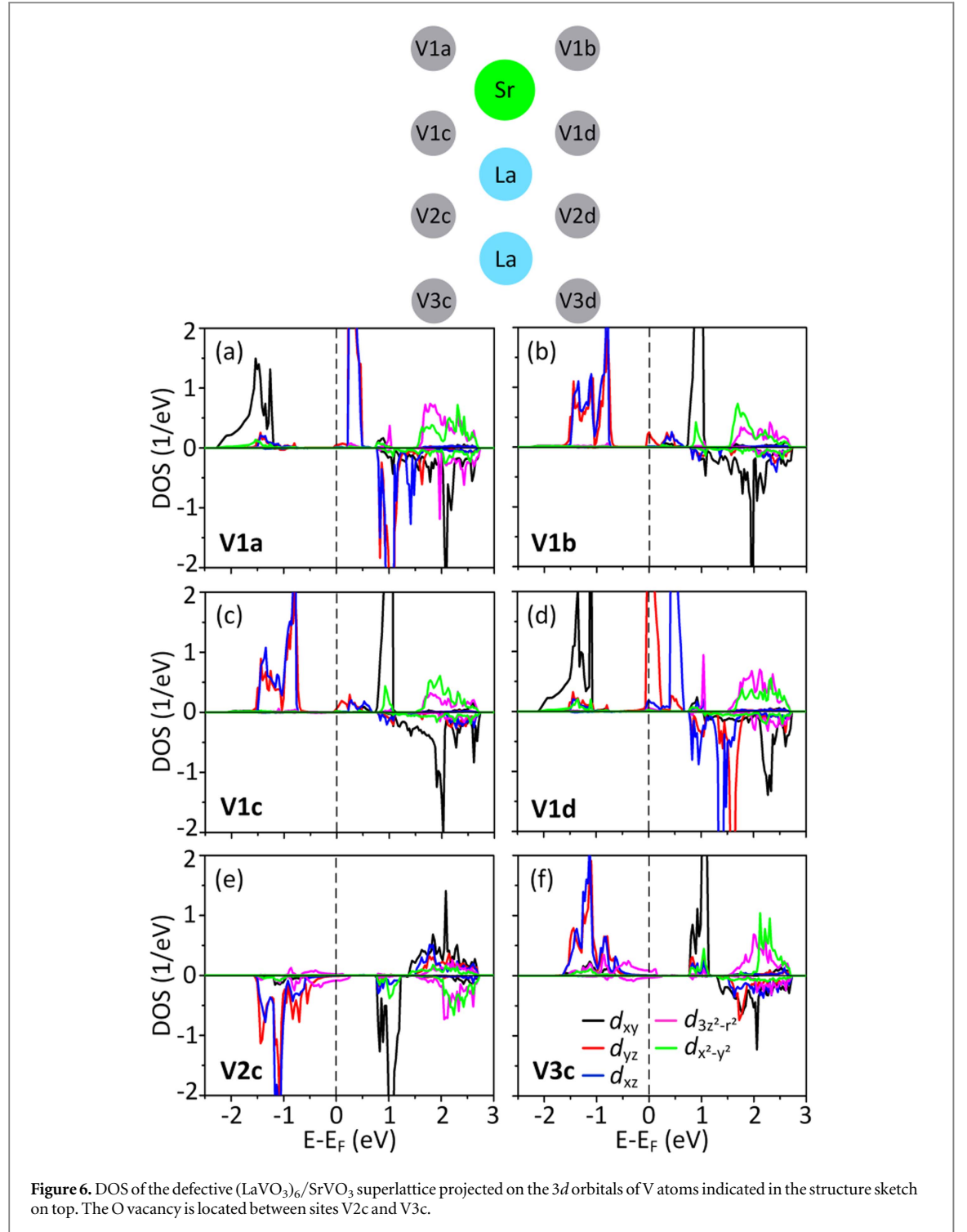
Figure 3. (a) Total DOS and (b) band structure of the (LaVO₃)₆/SrVO₃ superlattice with O vacancy in layer L3. Black and red lines in (b) denote spin majority and minority bands, respectively.

orbitals become partially occupied at sites V3c and V3d. The metallic character thus is induced by the interplay between the O vacancy and the interface, which, of course, is impossible in the case of defective bulk LaVO₃ due to the absence of V⁴⁺ ions (while a comparable situation is realized in La_{1-x}Sr_xVO₃ solid solutions with mixed V³⁺ and V⁴⁺ states and in appropriately doped LaVO₃, i.e., the discovered mechanism may play a role). As a consequence of the charge transfer, we find that the magnetic moment is reduced from 1.96 to 1.86 μ_B for sites V3c and V3d but enhanced from 1.10 to 1.46 μ_B for site V1d.

As second example for the metallic regime, we study an O vacancy between layers L2 and L3, which demonstrates that the described charge transfer phenomenon is not limited to OV_L but also occurs for OV_B. The metallic character of the superlattice is clearly visible in figure 5, and figure 6 indicates charge transfer from sites V2c and V3c (located next to the O vacancy) to the V⁴⁺ ion at site V1d. The magnetic moment turns out to be 1.30 μ_B at site V1d, 1.88 μ_B at site V2c, and 1.91 μ_B at site V3c. We note that site V2c (layer L2) is closer to the V⁴⁺ ion than site V3c (layer L3) so that the reduction of its magnetic moment (from 1.96 μ_B) is slightly more pronounced.

Turning to the semiconducting regime of the defective superlattice, compare figure 2, we address as example an O vacancy in layer L1, located between sites V1c and V1d. According to the total DOS and band structure, see figures 7(a) and (b), respectively, this defect conserves the semiconducting character of the superlattice but the band gap is reduced from 0.70 to 0.51 eV. In figure 8 we show the DOS projected on the 3d orbitals of the V atoms in layer L1. We find that the excess charge due to the O vacancy results in a 3d² configuration for site V1d,





see figure 8(d), while site V1a keeps its $3d^1$ configuration, see figure 8(a). The magnetic moments at sites V1c and V1d turn out to be both $1.96 \mu_B$, whereas those of the other V^{3+} ions remain at $1.82 \mu_B$.

4. Conclusion

We have studied the stability of O vacancies at different sites in the $(\text{LaVO}_3)_6/\text{SrVO}_3$ superlattice. It turns out that the formation energy decreases gradually from the bulk-like region of the superlattice towards the SrO layer (interface). An O vacancy in the bulk-like region leads to charge accumulation on the two neighboring V atoms as well as to charge transfer to the V^{4+} ions in the checkerboard pattern at the interface. As a consequence, partially filled bands are generated which give rise to a metallic character of the superlattice. This mechanism

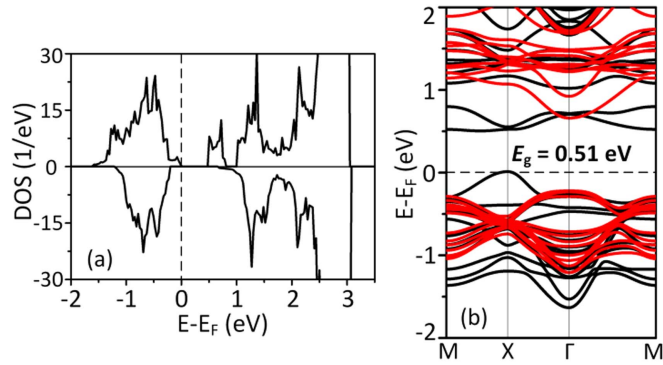


Figure 7. (a) Total DOS and (b) band structure of the $(\text{LaVO}_3)_6/\text{SrVO}_3$ superlattice with O vacancy in layer L1. Black and red lines in (b) denote spin majority and minority bands, respectively.

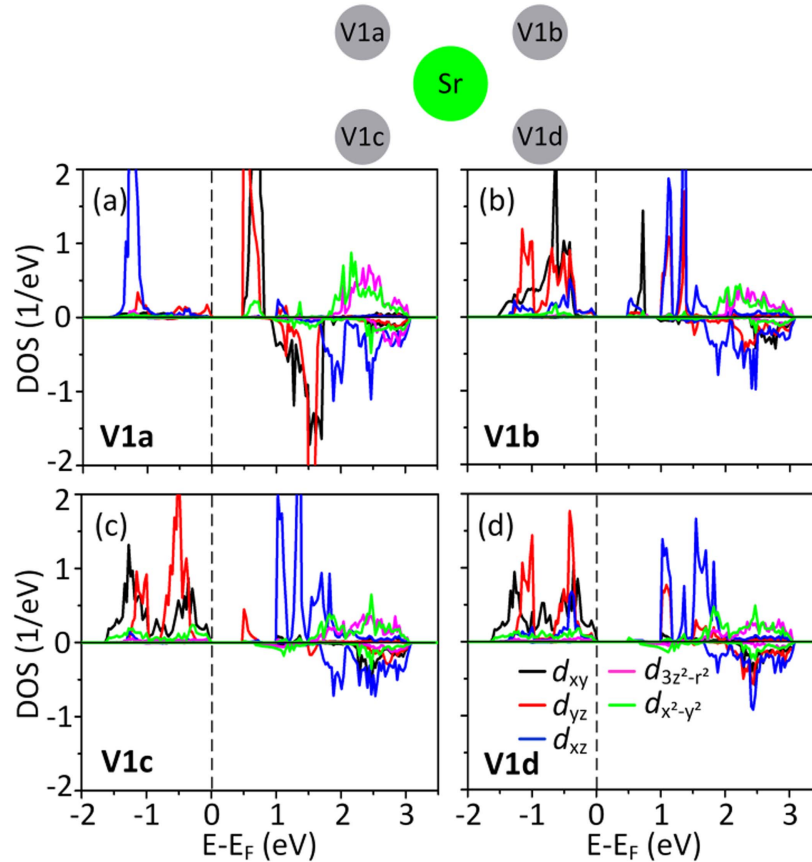


Figure 8. DOS of the defective $(\text{LaVO}_3)_6/\text{SrVO}_3$ superlattice projected on the $3d$ orbitals of V atoms indicated in the structure sketch on top. The O vacancy is located between sites V1c and V1d.

plays no role in the case of bulk LaVO_3 , since there are no V^{4+} ions that could accept additional charge. On the other hand, it may be speculated that the discovered mechanism becomes relevant, for example, for $\text{La}_{1-x}\text{Sr}_x\text{VO}_3$ solid solutions with mixed V^{3+} and V^{4+} states and for appropriately doped LaVO_3 . When the O vacancy is located within a range of not more than two VO_2 layers next to the SrO layer, surprisingly, the semiconducting state of the superlattice is conserved despite the O deficiency. This finding has been explained in terms of a perturbation of the $\text{V}^{3+}-\text{V}^{4+}$ checkerboard pattern that is present in the $(\text{LaVO}_3)_6/\text{SrVO}_3$ superlattice in the VO_2 layers next to the SrO layer. Instead of partial charge transfer, as in the case of bulk-like O vacancies, here V ions at the interface change their oxidation state fully from $4+$ to $3+$ and in that way are able to absorb the entire excess charge resulting from the O deficiency. The conservation of the semiconducting character is an immediate consequence of this observation.

Acknowledgments

The research reported in this publication was supported by funding from King Abdullah University of Science and Technology (KAUST). Financial support from the German Research Foundation (DFG) through TRR 80 is acknowledged.

ORCID iDs

Ulrich Eckern  <https://orcid.org/0000-0001-8917-9083>

Udo Schwingenschlögl  <https://orcid.org/0000-0003-4179-7231>

References

- [1] Mannhart J and Schlom D G 2004 Semiconductor physics: the value of seeing nothing *Nature* **430** 620–1
- [2] Santander-Syro A F *et al* 2011 Two-dimensional electron gas with universal subbands at the surface of SrTiO₃ *Nature* **469** 189–93
- [3] Kalinin S V, Borisevich A and Fong D 2012 Beyond condensed matter physics on the nanoscale: the role of ionic and electrochemical phenomena in the physical functionalities of oxide materials *ACS Nano* **6** 10423–37
- [4] Veal B W, Kim S K, Zapol P, Iddir H, Baldo P M and Eastman J A 2016 Interfacial control of oxygen vacancy doping and electrical conduction in thin film oxide heterostructures *Nat. Commun.* **7** 11892
- [5] Petrie J R, Mitra C, Jeon H, Choi W S, Meyer T L, Reboredo F A, Freeland J W, Eres G and Lee H N 2016 Strain control of oxygen vacancies in epitaxial strontium cobaltite films *Adv. Funct. Mater.* **26** 1564–70
- [6] Lin C and Demkov A A 2014 Consequences of oxygen-vacancy correlations at the SrTiO₃ interface *Phys. Rev. Lett.* **113** 157602
- [7] Shen J, Lee H, Valenti R and Jeschke H O 2012 *Ab initio* study of the two-dimensional metallic state at the surface of SrTiO₃: importance of oxygen vacancies *Phys. Rev. B* **86** 195119
- [8] Kubicek M, Cai Z, Ma W, Yildiz B, Hutter H and Fleig J 2013 Tensile lattice strain accelerates oxygen surface exchange and diffusion in La_{1-x}Sr_xCoO_{3-δ} *ACS Nano* **7** 3276–86
- [9] Pavlenko N, Kopp T, Tsymbal E Y, Sawatzky G A and Mannhart J 2012 Magnetic and superconducting phases at the LaAlO₃/SrTiO₃ interface: the role of interfacial Ti 3d electrons *Phys. Rev. B* **85** 020407
- [10] Pavlenko N, Kopp T, Tsymbal E Y, Mannhart J and Sawatzky G A 2012 Oxygen vacancies at titanate interfaces: two-dimensional magnetism and orbital reconstruction *Phys. Rev. B* **86** 064431
- [11] Liu Z Q *et al* 2013 Origin of the two-dimensional electron gas at LaAlO₃/SrTiO₃ interfaces: the role of oxygen vacancies and electronic reconstruction *Phys. Rev. X* **3** 021010
- [12] Ohtomo A and Hwang H Y 2004 A high-mobility electron gas at the LaAlO₃/SrTiO₃ heterointerface *Nature* **427** 423–6
- [13] Eckstein J N 2007 Oxide interfaces: watch out for the lack of oxygen *Nat. Mater.* **6** 473–4
- [14] Kalabukhov A, Gunnarsson R, Börjesson J, Olsson E, Claesson T and Winkler D 2007 Effect of oxygen vacancies in the SrTiO₃ substrate on the electrical properties of the LaAlO₃/SrTiO₃ interface *Phys. Rev. B* **75** 121404
- [15] Li L, Richter C, Mannhart J and Ashoori R C 2011 Coexistence of magnetic order and two-dimensional superconductivity at LaAlO₃/SrTiO₃ interface *Nat. Phys.* **7** 762–6
- [16] Salluzzo M *et al* 2013 Origin of interface magnetism in BiMnO₃/SrTiO₃ and LaAlO₃/SrTiO₃ heterostructures *Phys. Rev. Lett.* **111** 087204
- [17] Sheets W C, Mercey B and Prellier W 2007 Effect of charge modulation in (LaVO₃)_m(SrVO₃)_n superlattices on the insulator-metal transition *Appl. Phys. Lett.* **91** 192102
- [18] Lüders U, Sheets W C, David A, Prellier W and Frésard R 2009 Room-temperature magnetism in LaVO₃/SrVO₃ superlattices by geometrically confined doping *Phys. Rev. B* **80** 241102
- [19] Jeong D W *et al* 2011 Optical spectroscopy of the carrier dynamics in LaVO₃/SrVO₃ superlattices *Phys. Rev. B* **84** 115132
- [20] Boullay P *et al* 2011 Microstructure and interface studies of LaVO₃/SrVO₃ superlattices *Phys. Rev. B* **83** 125403
- [21] David A, Frésard R, Boullay P, Prellier W, Lüders U and Janolin P-E 2011 Structural transition in LaVO₃/SrVO₃ superlattices and its influence on transport properties *Appl. Phys. Lett.* **98** 212106
- [22] Tan H Y *et al* 2013 Mapping electronic reconstruction at the metal-insulator interface in LaVO₃/SrVO₃ heterostructures *Phys. Rev. B* **88** 155123
- [23] Dai Q, Lüders U, Frésard R, Eckern U and Schwingenschlögl U Electronic reconstruction in (LaVO₃)_m/SrVO₃ (*m* = 5, 6) superlattices *Adv. Mater. Interfaces* (<https://doi.org/10.1002/admi.201701169>)
- [24] Hu L *et al* 2014 Oxygen vacancies-induced metal-insulator transition in La_{2/3}Sr_{1/3}VO₃ thin films: role of the oxygen substrate-to-film transfer *Appl. Phys. Lett.* **105** 111607
- [25] Blöchl P E 1994 Projector augmented-wave method *Phys. Rev. B* **50** 17953–79
- [26] Kresse G and Joubert D 1999 From ultrasoft pseudopotentials to the projector augmented-wave method *Phys. Rev. B* **59** 1758–75
- [27] Kresse G and Hafner J 1993 *Ab initio* molecular dynamics for liquid metals *Phys. Rev. B* **47** 558–61
- [28] Kresse G and Hafner J 1994 *Ab initio* molecular-dynamics simulation of the liquid-metal-amorphous-semiconductor transition in germanium *Phys. Rev. B* **49** 14251–69
- [29] Kresse G and Furthmüller J 1996 Efficiency of *ab initio* total energy calculations for metals and semiconductors using a plane-wave basis set *Comput. Mater. Sci.* **6** 15–50
- [30] Kresse G and Furthmüller J 1996 Efficient iterative schemes for *ab initio* total-energy calculations using a plane-wave basis set *Phys. Rev. B* **54** 11169–86
- [31] Perdew J P, Burke K and Ernzerhof M 1996 Generalized gradient approximation made simple *Phys. Rev. Lett.* **77** 3865–8
- [32] Perdew J P, Burke K and Ernzerhof M 1997 Generalized gradient approximation made simple *Phys. Rev. Lett.* **78** 1396
- [33] Dudarev S L, Botton G A, Savrasov S Y, Humphreys C J and Sutton A P 1998 Electron-energy-loss spectra and the structural stability of nickel oxide: an LSDA+U study *Phys. Rev. B* **57** 1505–9
- [34] Arima T, Tokura Y and Torrance J B 1993 Variation of optical gaps in perovskite-type 3d transition-metal oxides *Phys. Rev. B* **48** 17006–9
- [35] Zhang L, Zhou X-F, Wang H-T, Xu J-J, Li J, Wang E G and Wei S-H 2010 Origin of insulating behavior of the *p*-type LaAlO₃/SrTiO₃ interface: polarization-induced asymmetric distribution of oxygen vacancies *Phys. Rev. B* **82** 125412